


Article

Assessment of Erosive Rainfall and Its Spatial and Temporal Distribution Characteristics: Case Study of Henan Province, Central China

Zhijia Gu ^{1,2} , Yuemei Li ^{1,2}, Shuping Huang ^{1,2}, Chong Yao ^{1,2,*}, Keke Ji ^{1,2}, Detai Feng ³, Qiang Yi ^{2,4} and Panying Li ^{2,4}

¹ School of Geographical Sciences, Xinyang Normal University, Xinyang 464000, China; guzhijia@xynu.edu.cn (Z.G.)

² North-South Transitional Zone Typical Vegetation Phenology Observation and Research Station of Henan Province, Xinyang 464000, China

³ Yunnan Key Laboratory of Soil Erosion Prevention and Green Development, Yunnan University, Kunming 650091, China

⁴ Soil and Water Conservation Monitoring Station of Henan Province, Zhengzhou 450008, China

* Correspondence: yaochong@xynu.edu.cn

Abstract: Erosive rainfall is essential for initiating surface runoff and soil erosion to occur. The analysis on its temporal and spatial distribution characteristics is crucial for calculating rainfall erosivity, predicting soil erosion, and implementing soil and water conservation. This study utilized daily rainfall observation data from 90 meteorological stations in Henan from 1981 to 2020, and conducted geostatistical analysis, M-K mutation test analysis, and wavelet analysis on erosive rainfall to reveal the spatiotemporal distribution characteristics over the past 40 years. Building on this foundation, the correlation between erosive rainfall, rainfall, and rainfall erosivity were further explored. The findings indicated that the average annual rainfall in Henan Province varied between 217.66 mm and 812.78 mm, with an average yearly erosive rainfall of 549.24 mm and a standard deviation of 108.32 mm. Erosive rainfall constitutes for 77% of the average annual rainfall on average, and the analysis found that erosive rainfall is highly correlated with rainfall volume. The erosive rainfall increased from northwest to southeast, and had the same spatial distribution characteristics as the total rainfall. The number of days with erosive rainfall was 20.5 days and the annual average sub-erosive rainfall was 26.86 mm. The average annual rainfall erosivity in Henan Province ranged from 1341.81 to 6706.64 MJ·mm·ha⁻¹·h⁻¹, averaging at 3264.63 MJ·mm·ha⁻¹·h⁻¹. Both the erosive rainfall and the rainfall erosivity are influenced by the monsoon, showing a unimodal trend, with majority of the annual total attributed to rainfall erosivity from June to September, amounting to 80%. The results can provide a basis for forecasting of heavy rainfall events, soil conservation and planning, ecological treatment, and restoration.

Keywords: erosive rainfall; spatiotemporal variation; rainfall erosivity; Henan Province



Academic Editor: Xiaosheng Qin

Received: 28 November 2024

Revised: 24 December 2024

Accepted: 26 December 2024

Published: 29 December 2024

Citation: Gu, Z.; Li, Y.; Huang, S.; Yao, C.; Ji, K.; Feng, D.; Yi, Q.; Li, P. Assessment of Erosive Rainfall and Its Spatial and Temporal Distribution Characteristics: Case Study of Henan Province, Central China. *Water* **2025**, *17*, 62. <https://doi.org/10.3390/w17010062>

Copyright: © 2024 by the authors. Licensee MDPI, Basel, Switzerland.

This article is an open access article distributed under the terms and conditions of the Creative Commons Attribution (CC BY) license (<https://creativecommons.org/licenses/by/4.0/>).

1. Introduction

Rainfall-induced water erosion is a significant contributor to soil erosion, rain falls into the surface through raindrops [1], and rainwater washes away the surface soil, resulting in the destruction of soil structure and the loss of organic matter at the surface [2]. The global hydrological cycle has been modified as a consequence of global warming in recent years, leading to an anticipated rise in both the frequency and intensity of extreme rainfall events

at global and regional scales [3–5]. Rainfall characteristics are important factors affecting soil and water loss [6–9], and there is a strong correlation that exists between splash erosion and runoff generation on slopes and rainfall characteristics [10]. Not all rainfall can cause soil erosion. Soil erosion occurs when the rainfall characteristics reach a certain critical standard, approaching or exceeding the critical value [11,12]. The critical value is called the erosive rainfall threshold [13]. The determination of the erosive rainfall standard is crucial for calculating rain erosion force and predicting soil loss accurately. In Universal Soil Loss Equation (USLE) and Revised Universal Soil Loss Equation (RUSLE), the erosive rainfall standard is formulated based on the intensity of the rainfall [14]. Rainfalls below 12.7 mm are not taken into account in the calculation of rainfall erosivity. However, it is still considered in the calculation when surpasses 6.4 mm within a 15-min interval.

There are substantial differences in soil erosion in China, with varying terrain and climate conditions at different regions, resulting in different standards for erosive rainfall. Some scholars have defined erosive rainfall in loess areas as a rainfall greater than $10 \text{ mm}\cdot\text{day}^{-1}$ [15], and $9.8 \text{ mm}\cdot\text{day}^{-1}$ and $9.2 \text{ mm}\cdot\text{day}^{-1}$ in Heilongjiang in Northeast China and Northeast Yunnan in Southwest China [16,17]. Scholars have classified erosive rainfall in the Xiao'anxi River Basin of the Yangtze River and the Loess Plateau by a rainfall $\geq 12.7 \text{ mm}$ per time [18–20]. Additionally, 14 mm is employed as the criterion for erosive rainfall in the Poyang Lake Basin [21]. In certain special landscape areas, such as the Karst landform area, a rainfall $\geq 30 \text{ mm}$ per time is employed as the standard for erosive rainfall [22]. The studies in the Karst Yellow Soil Mountain Erosion-Prone Region in Southwest China showed that the threshold for rainfall amounts was determined to be 12.66 mm for forest land, 10.57 mm for grassland, 9.94 mm for farmland, and 8.93 mm for fallow land [23]. It can be seen that the standards of erosive rainfall in different regions are also different due to different influencing factors such as geographical location, geomorphic features, and rainfall characteristics. The current rainfall $> 10 \text{ mm}\cdot\text{day}^{-1}$ or $12 \text{ mm}\cdot\text{day}^{-1}$ has been accepted by most scholars as the standard of erosion rainfall [24,25]. Chinese scholars usually used $12 \text{ mm}\cdot\text{day}^{-1}$ as the erosive rainfall threshold when calculating erosive rainfall based on daily rainfall [26].

The correlation between erosive rainfall and soil erosion is more closely related. Research indicated that rainfall-induced soil erosion varied significantly from year to year, with major storms accounting for the majority of overall erosion. Soil erosion caused by the most substantial rainfall event could account for 66.4% of the total annual erosion, with this figure surpassing 95% in a typical year. Among erosive rain events, half of the rainfall occurrences led to 96.8% of the overall soil loss [27]. With the escalation of global warming, frequent extreme rainfall events lead to severe soil erosion. The kinetic energy of intense raindrops surpasses that of typical rainfall occurrences [28–30]. Understanding and mastering the characteristics of regional rainfall and erosive rainfall has a guiding effect on regional soil and water conservation efforts.

The spatiotemporal distribution patterns of erosive rainfall have increasingly attracted the attention of researchers worldwide. Based on the analysis of erosion hazardous rainfall, the spatiotemporal characteristics of the trends in the frequency and volume of erosive rainfall in the European part of Russia (EPR) from 1966 to 2020 were studied [31]. Using the daily rainfall data collected from 71 meteorological stations in the Yellow River Basin in Shanxi Province from 2000 to 2016, spatial interpolation and other techniques were used to analyze the variation characteristics in temporal and spatial of erosive rainfall [32]. From 1961 to 2010, the erosion rainfall increased in majority areas within the upper reaches of the Yellow River basin, while decreased significantly in the Loess Plateau with serious soil erosion [33]. Another research found that erosive rainfall exhibited a noticeable decrease trend over the Loess Plateau after the extensive revegetation efforts from 2000 to 2015,

despite increased in total rainfall amount [34]. Based on daily rainfall data, the spatiotemporal changes in annual rainfall and erosive rainfall within Qinghai Province and its four ecological functional zones were studied [35]. Some researchers have used the method of trend and mutation analysis (Mann–Kendall test) to analyze the trend and mutation of rainfall and erosive rainfall in Tangtai area from 1960 to 2015 [36].

According to the 2023 China Soil and Water Conservation Bulletin, the area of soil erosion in Henan Province is 19,832 km², of which hydraulic erosion accounts for 93.65% [37]. Erosive rainfall is the primary contributor to water erosion in Henan and rainfall erosion recently played an important role. At present, there is a relative lack of systematic research on the spatiotemporal characteristics and changes of erosive rainfall in Henan [38]. Henan has encountered numerous historical heavy rainstorms. An extraordinary heavy rainstorm, with a peak 24-h rainfall of 1060.3 mm, occurred between 4th and 8th August 1975, which lead to catastrophic flooding, resulting in 26,000 fatalities and leaving approximately 10 million people without proper shelter [39,40]. In July 2021, Henan Province experienced another record-breaking rainfall event, with a maximum 24-h (1-h) rainfall of 624 mm (201.9 mm) record at Zhengzhou Weather Station. Unexpected heavy rainfall resulted in 398 fatalities and economic losses amounting to 120.06 billion RMB [41,42]. At present, there is a dearth of systematic study on the temporal and spatial attributes and dynamic changes of erosive rainfall in Henan.

Exploring the spatiotemporal distribution patterns of erosive rainfall and rainfall erosivity in Henan Province can provide a foundation for forecasting heavy rainfall events, preventing and controlling soil erosion, ecological treatment and restoration, and soil and water conservation planning in the study area. Long time series and high density meteorological stations are the key to analyzing spatial and temporal characteristics of erosive rainfall. Daily rainfall data of Henan Province after 1981 were cited from the first national water conservancy survey conducted in 2011. Therefore, the quality and accuracy of the data can serve the research purpose of this study. Using the daily rainfall data from 90 meteorological stations in Henan, this study analyzes the erosive rainfall from 1981 to 2020. In this study, we pursued the following objectives: (1) analyzing the temporal dynamic trends of erosive rainfall in Henan Province based on wavelet analysis and M-K mutation analysis; (2) to analyze the spatial arrangement of erosive rainfall based on geostatistical analysis; (3) and to identify the spatiotemporal changes in rainfall erosivity and its correlation with erosive rainfall in Henan. The objective is to offer a reference for soil erosion prevention and control in different periods within the research area.

2. Materials and Methods

2.1. Study Area

Henan is in the middle and lower sections of the Yellow River in central China, with geographical coordinates of 31°23′–36°22′ N and 110°21′–116°39′ E, and is located in the transition zone between the second and third stages of China. The elevation is higher in the western regions and lower in the eastern area, resulting in a ladder-like terrain distribution from west to east. Situated in the northern subtropical warm temperate zone, humid, and semi humid climate, Henan has obvious transitional climate characteristics and distinct four seasons, which belongs to monsoon climate. The average annual temperature varies between 12 °C and 16 °C, with extreme maximum and minimum temperatures recorded at 44.2 °C and −21.7 °C, respectively [43]. The annual rainfall is between 532.5 and 1380.6 mm, and the rainfall is predominantly concentrated in summer and autumn months, making up 60–70% of the annual rainfall [44]. In the mountainous and hilly areas of Henan, the Funiu Mountain, the east foot of Taihang Mountain, and the north side of Dabie Mountain are the centers of rainfall. When the rainstorm comes, the slope in hilly areas is steep and the

water flow speed is accelerated, which easily causes sudden floods and serious soil erosion in mountainous and hilly areas.

Within the framework of national soil and water conservation regionalization, Henan includes five secondary regions: Taihang Mountain Hilly Area, Mountainous and Hilly Area of Southwest Henan, North China Plain Area, Dabie-Tongbai Mountain Hilly Area, and Qinba Mountain Area [24]. Among them, the Taihang Mountain Hilly Area, Mountainous and Hilly Area of Southwest Henan, and the North China Plain Area secondary areas belong to the Northern Rock area. The Dabie-Tongbai Mountain Hilly Area belongs to the southern red soil area. The Qinba Mountain Area belongs to the southwestern purple soil area. Among the 90 meteorological stations collected in this study, three of them are situated in the Taihang Mountain Hilly Area, twenty-eight of them are situated in the hilly area of southwestern Henan, forty-six of them are located in the North China Plain Area, twelve of them are situated in the hilly area of Dabie-Tongbai Mountain Hilly Area, and one of them is situated in the mountain area of Qinba Mountain Area (Figure 1).

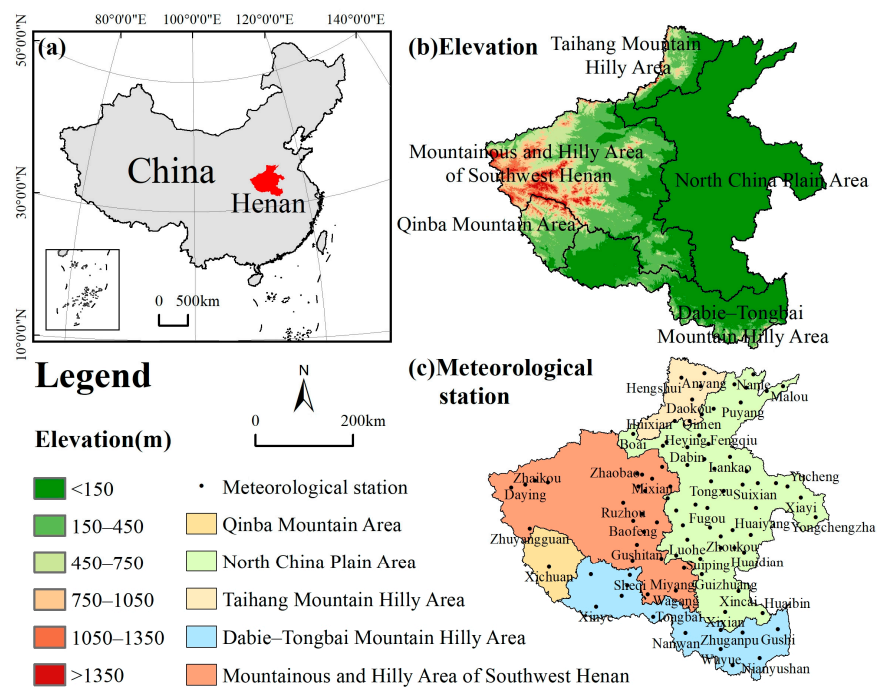


Figure 1. The location of the study area in China (a), elevation of the study area (b), and spatial distribution of meteorological stations in five national soil and water conservation zones (c).

2.2. Methodology

2.2.1. Calculation of Annual Erosive Rainfall

The basic data used in this study are the daily rainfall data from 90 meteorological stations in Henan from 1981 to 2020. In this paper, the standard for erosive rainfall is set as a daily rainfall of at least 10 mm. The expression for calculating the annual rainfall amount is as follows [24]:

$$Py_{12} = \sum_{i=1}^n Pd_{10}(i) \tag{1}$$

where Py_{12} represents the annual volume of erosive rainfall; Pd_{10} represents the daily erosive rainfall amount; and n represents the number of days with erosive rainfall in a year.

2.2.2. Kriging Interpolation Method

Kriging interpolation is an important tool for geographic analysis. It was based on the measurement of geographic map data, mostly based on the relationship between the

geographical locations of sampling points in the region. Compared with other methods, kriging interpolation is more suitable for the numerical analysis of this region, and the results are more accurate. The most common is the kriging interpolation method based on the traditional spherical function [45]. In this study, different types of interpolation transformations are analyzed in terms of the interpolation of semi-variance function. According to the spatial interpolation of the survey in the region, the interpolation of erosive rainfall and rainfall erosivity within the study area was obtained.

2.2.3. Mann–Kendall Mutation Detection

The Mann–Kendall test is a non-parametric method. It is relatively simple to calculate in geographic information analysis. It is calculated and analyzed by inverse sequence (UB) and constructing positive sequence (UF). The curves of UB and UF determine the variation trend and mutation characteristics [46]. The M-K mutation test can indicate mutation points in geography, and the expression of extreme climate trends is as follows:

$$S = \sum_{i=1}^{n-1} \sum_{j=i+1}^n \operatorname{sgn}(x(j) - x(i)) \quad (2)$$

$$\operatorname{sgn}(x(j) - x(i)) = \begin{cases} 1, & x(i) > x(j) \\ 0, & x(i) = x(j) \\ -1, & x(i) < x(j) \end{cases} \quad (3)$$

$$E(S) = 0 \quad (4)$$

$$\operatorname{Var}(S_k) = \frac{1}{18} \left[n(n-1)(2n+5) - \sum_{l=1}^m k_l(k_l-1)(2k_l+5) \right] \quad (5)$$

$$Z = \begin{cases} (S-1)/\sqrt{\operatorname{Var}(S_k)}, & S > 0 \\ 0, & S = 0 \\ (S+1)/\sqrt{\operatorname{Var}(S_k)}, & S < 0 \end{cases} \quad (6)$$

where $x(j)$ and $x(i)$ represent the erosive rainfall of years j and i , n is the length of time series, and sgn is the sgn function. $E(S)$ and $\operatorname{Var}(S_k)$ are the average and variance of the cumulative number S_k . The statistic Z follows a standard normal distribution. It represents an increasing trend when the value of Z is greater than 0 and conversely for a decreasing trend.

2.2.4. Wavelet Analysis

Wavelet transform is a transformation of windowed Fourier and Fourier analysis, which achieves time frequency transformation through translation and scaling. It is frequently employed for frequency analysis of time series and is suitable for time-frequency analysis in meteorology and hydrology [47]. This study uses Morlet wavelet analysis as the mother function for wavelet analysis and the specific expression is as follows:

$$\varphi(t) = e^{i\omega t} e^{-t^2/2} \quad (7)$$

where i is an imaginary unit, and t is a time variable. ω is defined as a dimensionless constant, and a value greater than or equal to 5 is considered an allowed range. This value represents the sequence cycle of hydrological data extraction and the degree of energy intensity in the oscillation cycle. We use the red noise standard to detect the significance of wavelet power spectrum. If the value of a exceeds the theoretical power spectrum Q , then this period is considered valid.

$$Q = \frac{\sigma^2 P_\alpha \chi_n^2}{n} \quad (8)$$

$$P_\alpha = \frac{1 - \alpha^2}{1 + \alpha^2 - 2\alpha \cos(2\pi\Delta t/1.033\alpha)} \quad (9)$$

where σ^2 is the variance of the data sequence; the changes in the data sequence X_n^2 are the squared values of the n degrees of freedom at the significance level; P_α is the standard red noise spectral density of the data sequence at the time interval. Δt is selected as the item, and 1 is the autocorrelation coefficient of the sequence delay.

2.2.5. Calculation of Rainfall Erosivity

In this study, the daily rainfall erosivity model was utilized for the computation of rainfall erosivity [25]. The specific mathematical expression is as follows:

$$R_i = \alpha \sum_{j=1}^k P_j^\beta \quad (10)$$

This study took daily rainfall ≥ 10 mm as the standard for classifying erosive rainfall, otherwise it is calculated as 0. Here, α and β are undetermined parameters of the model, R_i represents the rainfall erosivity for the i th half-month ($\text{MJ}\cdot\text{mm}\cdot\text{ha}^{-1}\cdot\text{h}^{-1}$), k is the number of rainy days within that half-month, and P_j is the erosive daily rainfall (in mm) on the j th day of that half-month. The calculation formula is as follows:

$$\begin{aligned} \beta &= 0.8363 + \frac{18.177}{Pd_{10}} + \frac{24.455}{Py_{10}} \\ \alpha &= 21.586\beta^{-7.1891} \end{aligned} \quad (11)$$

where Pd_{10} represents the average daily rainfall for days with rainfall ≥ 10 mm; Py_{10} represents the annual average rainfall for days with rainfall ≥ 10 mm.

3. Results

3.1. Erosive Rainfall and Its Spatial Distribution Characteristics

The characteristics of the two rainfalls in Henan from 1981 to 2020 were analyzed, and the annual erosive rainfall in the study area was in the range from 217.66 mm in 2012 to 812.78 mm in 2000, with an average yearly erosive rainfall of 549.24 mm and a standard deviation of 130.11 mm, accounting for 77% of the annual average rainfall (Table 1). The annual rainfall was 290.71 mm in 2012 and 1053.64 mm in 2003, with an average annual rainfall of 717.86 mm and standard deviation of 130.59 mm. An analysis of the annual erosive rainfall in the five soil and water conservation zones of Henan revealed that among these five zones, the Dabie-Tongbai Mountain Hilly Area had the highest erosive rainfall, total rainfall, average annual number of erosive rainfall days, and average annual erosive rainfall. The average annual erosive rainfall, average annual rainfall, and average annual erosive rainfall days in the hilly area of Taihang Mountain Hilly Area were the lowest among the five soil and water conservation zones. In the southwestern mountainous and hilly areas of Henan and the North China Plain Area, the rainfall conditions are relatively similar. The North China Plain Area receives more rainfall overall. In terms of average daily erosive rainfall volume, the North China Plain Area ranked highest among the five soil and water conservation regions, while the Taihang Mountain Hilly Area had the lowest average erosive rainfall volume. The erosive rainfall in Henan generally showed an increasing trend from northwest to southeast from 1981 to 2020 (Figure 2a). The distribution characteristics of annual average erosive rainfall are basically the same as those of annual rainfall.

Table 1. Rainfall characteristics in the soil and water conservation regions of Henan Province.

Area	Annual Rainfall/mm	Annual Erosive Rainfall/mm	Proportion of Erosive Rainfall/%	Average Annual Erosive Rainfall Days/d	Average Daily Erosive Rainfall/mm
Taihang Mountain Hilly Area	553.87 ± 24.83	416.87 ± 13.84	75	15.3 ± 0.9	27.34 ± 1.35
Mountainous and Hilly Area of Southwest Henan	682.34 ± 141.16	510.61 ± 125.10	75	19.3 ± 3.7	26.43 ± 2.28
North China Plain Area	701.30 ± 166.95	550.04 ± 148.87	78	19.4 ± 4.0	28.29 ± 3.98
Dabie-Tongbai Mountain Hilly Area	916.56 ± 180.74	720.37 ± 158.44	79	25.8 ± 4.5	27.97 ± 1.63
Qinba Mountain Area	735.24	548.31	75	22.6	24.26
Mean value of Henan	717.86 ± 130.59	549.24 ± 108.32	77	20.5 ± 3.94	26.86 ± 1.62

Note: The values before and after the symbol “±” in the table are the mean and standard deviation, respectively.

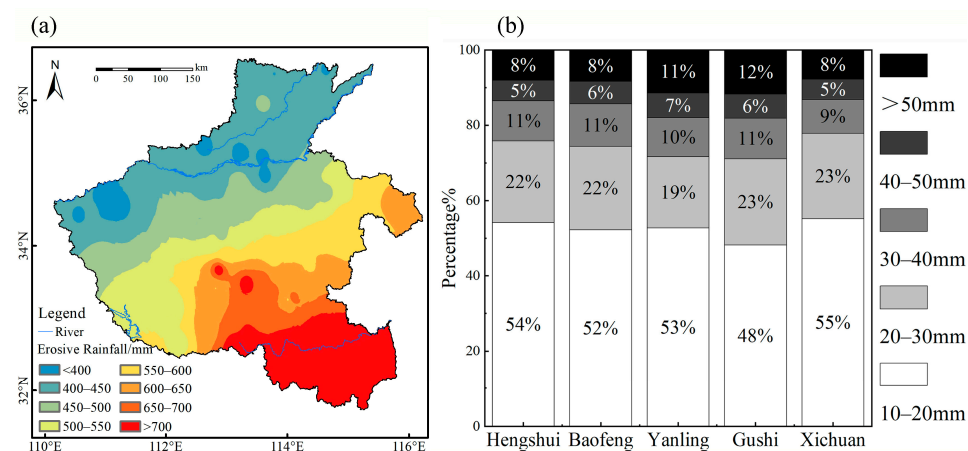


Figure 2. Spatial distribution of annual average erosive rainfall from 2000 to 2020 (a) and proportion of erosive rainfall in each soil and water conservation zone (b).

To further analyze the change trend of erosive rainfall in Henan, five representative meteorological stations were selected for quantitative analysis. They are Hengshui meteorological station in Taihang Mountain Hilly Area, Baofeng meteorological station in Mountainous and Hilly Area of Southwest Henan, Yanling in North China Plain Area, Gushi meteorological station in Dabie-Tongbai Mountain Hilly Area, and Xichuan meteorological station in Qinba Mountain Area. As depicted in Figure 2b, the proportion of past erosive rainfall at the five stations showed that the erosive rainfall of 10–20 mm in Henan accounted for about half of the total erosive rainfall. Compared to the other three regions, Gushi and Yanling, located in the southeastern part of Henan, indicated an increase in erosive rainfall exceeding 30 mm, accounting for 29% and 28% of the annual erosive rainfall. In Hengshui, Baofeng, and Xichuan, the erosive rainfall of more than 30 mm accounted for 24%, 25%, and 22%, respectively. The analysis of the days of erosive rainfall at five stations showed that the days of erosive rainfall at Hengshui station in the Taihang Mountain Hilly Area were only 16.5 days, while those at Baofeng, Yanling, Gushi, and Xichuan were 19.7 days, 19.7 days, 19.5 days, 28.1 days, and 22.6 days.

3.2. Analysis of Temporal Variation of Erosive Rainfall

3.2.1. Annual Variation of Erosive Rainfall

Located in central China, Henan was affected by the monsoon climate, with single peak rainfall and erosive rainfall, which have obvious seasonal characteristics. Rainfall and erosive rainfall are mainly concentrated in June–September and is relatively small from January to April (next year). From the perspective of warm and cold seasons, the erosive

rainfall in cold season is 49.32–175.99 mm and that in warm season is 366.05–540.9 mm. Among them, the proportion of erosive rainfall in the hilly region of Taihang Mountain Hilly Area is higher in warm season, accounting for 88%, and it is lower in the cold season, accounting for only 12%. The proportion of erosive rainfall in the hilly region of Dabie-Tongbai Mountain Hilly Area is 75% in the warm season and 25% in the cold season. The proportion of erosive rainfall in Qinba Mountain Area, North China Plain Area, and Mountainous and Hilly Area of Southwest Henan is 78%, 81%, and 82%, respectively, in the warm season, and the proportion of erosive rainfall in the cold season is 22%, 19%, and 18%, respectively (Table 2). Comparing the five soil and water conservation divisions, it was found that the erosive rainfall is relatively concentrated in the Taihang Mountain Hilly Area in the northwest of Henan, and relatively scattered in the Dabie-Tongbai Mountain Hilly Area near the southeast.

Table 2. Erosive rainfall characteristics in the soil and water conservation regions of Henan.

Area	Warm Season Erosive Rainfall		Cold Season Erosive Rainfall	
	Rainfall/mm	Proportion/%	Rainfall/mm	Proportion/%
Taihang Mountain Hilly Area	366.85 ± 16.19	88	50.02 ± 3.80	12
Mountainous and Hilly Area of Southwest Henan	418.70 ± 92.75	82	91.91 ± 40.72	18
North China Plain Area	445.53 ± 96.48	81	104.51 ± 54.54	19
Dabie-Tongbai Mountain Hilly Area	540.28 ± 96.42	75	180.09 ± 66.39	25
Qinba Mountain Area	427.68	78	120.63	22
Mean value of Henan	444.88 ± 63.63	81	104.36 ± 45.19	19

Note: The values before and after the symbol “±” in the table are the mean and standard deviation, respectively.

By analyzing the erosive rainfall in Henan for many years by month, it is found that the erosive rainfall in July and August accounts for 25% and 20% of the annual erosive rainfall, respectively (Figure 3). In addition, the erosive rainfall in the hilly area of Taihang Mountain Hilly Area is concentrated, and in July, its erosive rainfall even exceeds that in the hilly area of mountains in western Henan and Qinba Mountain Area. The influence of geographical location on erosive rainfall lies in the annual distribution of rainfall. The annual rainfall and erosive rainfall in Dabie-Tongbai Mountain Hilly Area near the warm and humid areas are relatively uniform, and the annual rainfall and erosive rainfall are relatively concentrated in the hilly area of Taihang Mountain Hilly Area near the north.

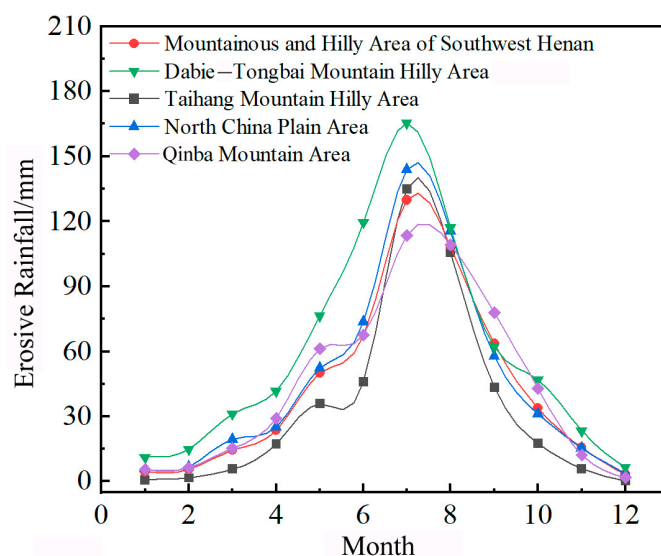


Figure 3. Monthly erosive rainfall in Henan Province from 1981 to 2020.

3.2.2. Periodic Analysis and Mutation Analysis

Wavelet analysis was applied to investigate the rainfall erosivity climate date in Henan for 40 years (Figure 4). The real component of Morlet wavelets can indicate the cyclic fluctuations of climate at various scales and the wavelet variance can divide the main period within the time series. In this study, the erosive rainfall in Henan from 1980 to 2020 is analyzed by wavelet analysis. The analysis showed that the erosive rainfall in Henan had a periodicity of 2–4 years, 9 years, 11 years, and 29–31 years, and the highest peak value was 30 years. Among them, 30 years stood out as the primary period of erosive rainfall change in Henan, and 3 years, 9 years, and 11 years were the second to fourth main periods. The periodic changes of erosive rainfall at all scales in Henan were relatively stable over the past 40 years.

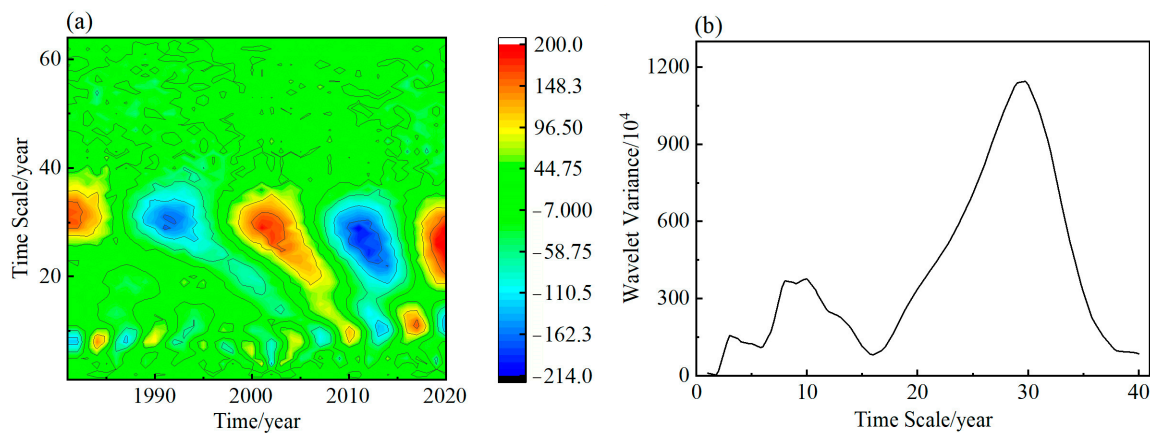


Figure 4. The wavelet transform coefficient of erosive rainfall (a) and wavelet variance of erosive rainfall (b).

Mann–Kendall mutation analysis of erosive rainfall in Henan from 1981 to 2020 was applied (Figure 5). The findings indicated that there was a significant spike in annual erosive rainfall in 1985. The UF curve was negative from 1985 to 2003, during which time the annual erosive rainfall revealed a downward trend and the UF value gradually increased from 2004 to a positive value, at which time the annual erosive rainfall exhibited an upward trend. But it turned negative again after 2010. Through wavelet analysis and M–K mutation analysis of Henan, it was found that the erosive rainfall had certain interannual and periodic changes. Wavelet analysis can reflect the periodic changes of erosive rainfall with different scales, which had certain positive significance for planning soil and water conservation measures in Henan.

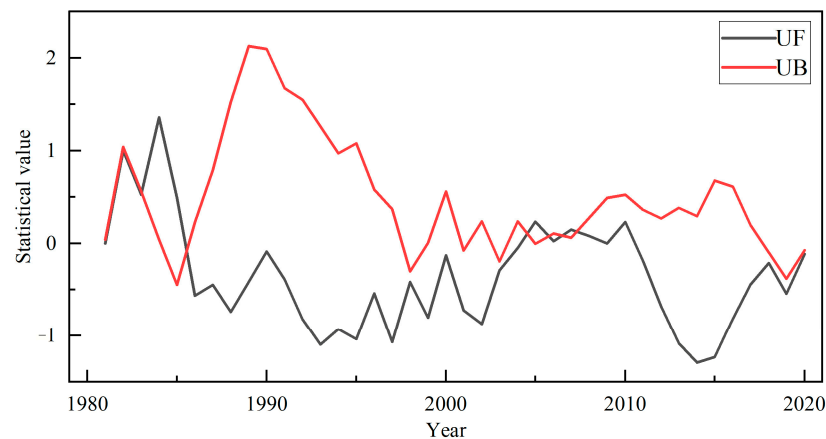


Figure 5. M–K mutation test of annual erosive rainfall in Henan Province from 1981 to 2020.

3.2.3. Temporal and Spatial Variation Characteristics of Rainfall Erosivity

By analyzing the rainfall erosivity in Henan from 1981 to 2020, the annual rainfall erosivity in the past 40 years was $3264.63 \text{ MJ}\cdot\text{mm}\cdot\text{ha}^{-1}\cdot\text{h}^{-1}$, changing between $1341.81 \text{ MJ}\cdot\text{mm}\cdot\text{ha}^{-1}\cdot\text{h}^{-1}$ and $6706.64 \text{ MJ}\cdot\text{mm}\cdot\text{ha}^{-1}\cdot\text{h}^{-1}$. The C_v value of rainfall erosivity is 0.32, indicating that its dispersion is obvious and rainfall erosivity fluctuates greatly (Table 3). The correlation analysis between rainfall erosivity, rainfall, and erosive rainfall indicated that the R^2 of erosive rainfall to rainfall erosivity was 0.83 and the R^2 of rainfall to rainfall erosivity was 0.78. Rainfall erosivity in Henan was significantly affected by erosive rainfall, which reached the maximum in warm season and was relatively small in cold season.

Table 3. Comparison of annual average total rainfall (mm), annual average erosive rainfall (mm), and annual average rainfall erosivity ($\text{MJ}\cdot\text{mm}\cdot\text{ha}^{-1}\cdot\text{h}^{-1}$) in Henan Province.

Index	Annual Average	Maximum (Year)	Minimum (Year)	Extremal Ratio	Coefficient of Variation
Total Rainfall	719.57	1053.64 (2003)	290.71 (2012)	2.62	0.21
Erosive Rainfall	549.24	812.78 (2000)	217.66 (2012)	2.73	0.24
Rainfall Erosivity	3264.63	6706.64 (2000)	1341.81 (2012)	4.00	0.32

By comparing the multi-year rainfall, erosive rainfall, and rainfall erosivity in Henan, it was observed that the annual rainfall erosivity had great dispersion and the extreme value ratio reached 4.0. The variation coefficient of average annual rainfall was the smallest (0.21). The extreme value ratio was 2.62. The standard deviation of erosive rainfall was 132.98mm, which is the smallest of the three indexes, indicating that the interannual variation of erosive rainfall is relatively stable compared with rainfall and rainfall erosivity.

Rainfall erosivity is significantly affected by rainfall and erosive rainfall. It is significantly affected by seasonal changes, which is unimodal. According to the analysis of rainfall erosivity in Henan, the rainfall erosivity generally demonstrated a rising pattern from northwest to southeast. However, due to the high concentration of rainfall in warm season in the Taihang Mountain Hilly Area, the rainfall erosivity in July can surpass that in the Mountainous and Hilly Area of Southwest Henan, the North China Plain Area, and Qinba Mountain Area.

4. Discussion

4.1. Relationship Between Erosive Rainfall and Annual Rainfall

Pearson correlation analysis was made between the average rainfall and the average erosive rainfall in Henan for many years, and the correlation coefficient between them was 0.989 (significantly correlated at the level of 0.01), indicating that erosive rainfall was significantly affected by rainfall (Figure 6). Affected by geographical location, topography, and other factors, rainfall generally rises from the northwest to the southeast. The maximum and minimum values of the average erosive rainfall in Henan from 1981 to 2020 are 812.78 mm and 217.66 mm, respectively. The erosive rainfall is obviously affected by rainfall, especially by seasons, mainly in warm seasons. Hence, it is necessary to strengthen soil and water conservation from June to September and pay attention to the occurrence of flood.

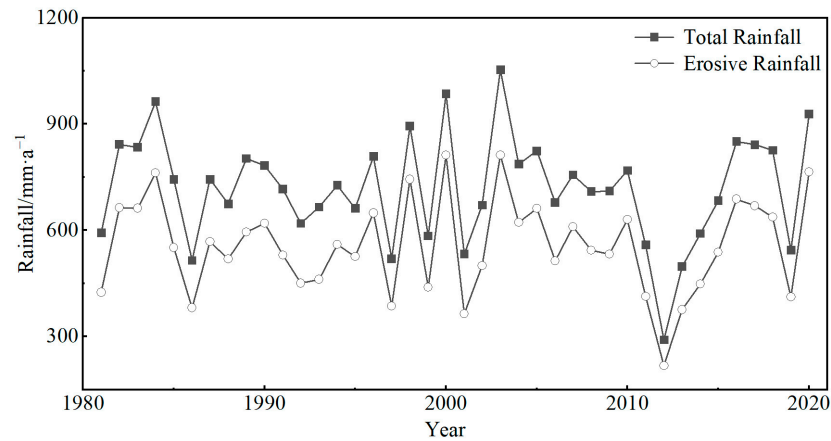


Figure 6. Changes of total rainfall and erosive rainfall in Henan from 1981 to 2020.

4.2. Relationship Between Erosive Rainfall and Rainfall Erosivity

Based on the linear fitting analysis of erosive rainfall and rainfall erosivity, it is concluded that erosive rainfall had a more significant impact on rainfall erosivity than rainfall. Correlation analysis of rainfall erosivity, annual rainfall, and erosive rainfall indicated that the correlation between rainfall and erosive rainfall was 0.884 (significantly correlated at 0.01 level), while the correlation between erosive rainfall and imminent erosive rainfall was 0.912 (significantly correlated at 0.01 level). Rainfall erosivity rose from the northwest to the southeast, and had the same spatial distribution pattern with the erosive rainfall (Figure 7).

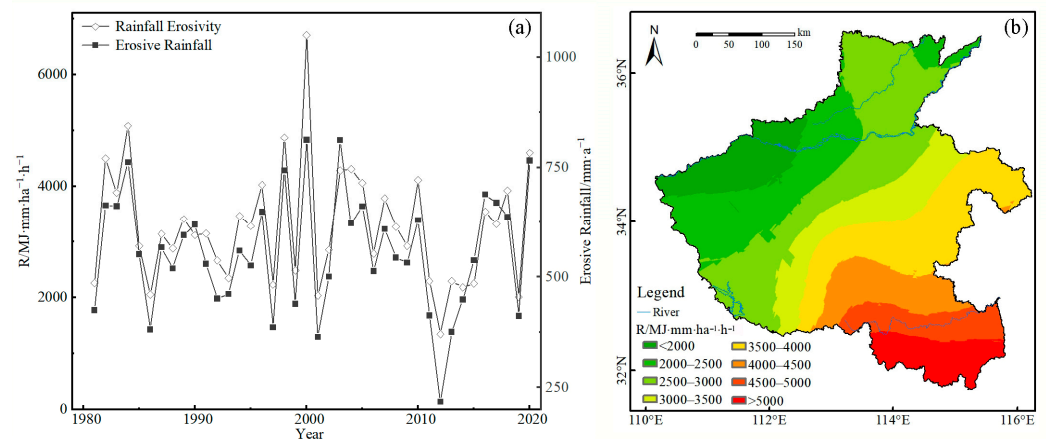


Figure 7. Changes of rainfall erosivity and erosive rainfall from 1981 to 2020 (a) and spatial distribution of rainfall erosivity in Henan from 1981 to 2020 (b).

The fitting results of erosive rainfall and rainfall erosivity are relatively significant (Figure 8). In recent years, with the ongoing strengthening of soil and water conservation, the severity of soil erosion has been reduced and extensive prevention and control has achieved certain effects. From the geographical point of view, the rainfall erosivity in Henan generally showed an increasing trend from northwest to southeast. Rainfall erosivity was strongly correlated with rainfall intensity and rainstorm days. The increase of rainfall, rainfall intensity, and rainfall days further improves rainfall erosivity, especially in mountainous and hilly areas; the problem of soil erosion caused by water erosion still exists. From the time point of view, the rainfall in Henan Province was mainly concentrated in the warm season, accounting for 81% of the total rainfall in the whole year. There are many rainstorm days in summer and autumn, and the rainfall erosivity is large, which is the high-incidence period of geological disasters such as floods and landslides. Special consideration should be given to the management of cultivated land in high-incidence

areas, increasing the conversion of farmland to forests and grasslands, improving the vegetation coverage, and improving the soil and water conservation capacity.

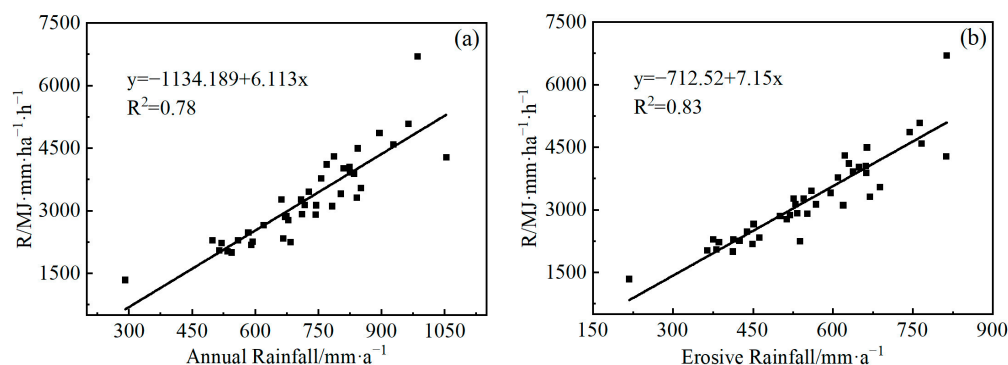


Figure 8. Linear fitting of rainfall erosivity to annual rainfall from 1981 to 2020 (a) and erosive rainfall from 1981 to 2020 (b).

5. Conclusions

Further exploration of spatiotemporal variation characteristics of erosive rainfall and its relationship with total rainfall and rainfall erosivity still needs to be promoted. Therefore, based on geostatistical analysis, M-K mutation test analysis, and wavelet analysis, daily rainfall observation data from 90 meteorological stations in Henan Province from 1981 to 2020 were selected to detect the spatiotemporal distribution characteristics over the past 40 years. The conclusions of the research are as follows:

1. From 1981 to 2020, the annual erosive rainfall in Henan ranged from 217.66 mm to 812.78 mm, with the average erosive rainfall of 549.24 mm, accounting for 77% of the total average rainfall. Overall, the erosive rainfall exhibited a rising trend from the northwest to the southeast, averaging 20.5 d of erosive rainfall every year.
2. The erosive rainfall in the research area showed a single peak trend during 1981–2020 and the maximum erosive rainfall occurred in July. The erosive rainfall in warm season (from June to September) makes up 81% of the annual erosive rainfall. Through wavelet analysis, it was found that the erosive rainfall in had a primary cycle of 30 years and cycle of 3 years, 9 years, and 11 years.
3. Based on the analysis of the correlation of rainfall erosivity, total rainfall, and erosive rainfall, erosive rainfall plays a very important role to affect rainfall erosivity. The annual rainfall erosivity in Henan Province changed from 1341.81 to 6706.64 MJ·mm·ha⁻¹·h⁻¹, and had a more significant correlation with erosive rainfall than that of total rainfall. In addition, the rainfall erosivity increased from northwest to southeast and had the same spatial distribution pattern as the erosive rainfall.
4. Analyzing the spatiotemporal distribution patterns of erosive rainfall and rainfall erosivity in Henan Province can provide a basis for forecasting of heavy rainfall events, preventing and controlling soil erosion, ecological treatment and restoration, and soil conservation planning. In recent years, with the frequent occurrence of extreme precipitation, extreme heavy rainfall is the major reason for severe soil erosion in the region. Research on the contribution of extreme rainfall to erosive rainfall should be strengthened.

Author Contributions: Conceptualization, Z.G. and Y.L.; methodology, Z.G. and S.H.; software, C.Y.; validation, Q.Y., Y.L. and P.L.; formal analysis, D.F.; investigation, K.J.; resources, Q.Y.; data curation, P.L.; writing—original draft preparation, Y.L.; writing—review and editing, Z.G.; visualization, Q.Y.; supervision, Y.L.; project administration, Z.G.; funding acquisition, Y.L. and D.F. All authors have read and agreed to the published version of the manuscript.

Funding: This research was funded by Key Research Projects of Higher Education Institutions in Henan Province, grant number 25A170004, 25A170007, Natural Science Foundation of Henan, grant number 232300420444, and Nanhu Scholars Program for Young Scholars of XYNU, grant number 2019046.

Data Availability Statement: The data that support the findings of this study are available on request from the corresponding author, [C.Y.], upon reasonable request.

Conflicts of Interest: The authors declare no conflicts of interest.

References

1. Wang, W.Z.; Jiao, J.Y. Quantitative evaluation on factors influencing soil erosion in China. *Bull. Soil Water Conserv.* **1996**, *16*, 1–20. (In Chinese) [[CrossRef](#)]
2. Li, Z.J.; Liu, J.Y.; Wang, H.J. Study on the characteristics of soil and water loss on the slopes in Northern Rocky Mountain area. *Res. Soil Water Conserv.* **2024**, *31*, 1–9. (In Chinese)
3. Tabari, H. Climate change impact on flood and extreme precipitation increases with water availability. *Sci. Rep.* **2020**, *10*, 13768. [[CrossRef](#)] [[PubMed](#)]
4. Domínguez-Tuda, M.; Gutiérrez-Jurado, H.A. Global analysis of the hydrologic sensitivity to climate variability. *J. Hydrol.* **2021**, *603*, 126720. [[CrossRef](#)]
5. Kendon, E.J.; Fischer, E.M.; Short, C.J. Variability conceals emerging trend in 100yr projections of UK local hourly rainfall extremes. *Nat. Commun.* **2023**, *14*, 1133. [[CrossRef](#)] [[PubMed](#)]
6. Huo, J.; Yu, X.; Liu, C.; Chen, L.; Zheng, W.; Yang, Y.; Tang, Z. Effects of soil and water conservation management and rainfall types on runoff and soil loss for a sloping area in North China. *Land Degrad. Dev.* **2020**, *31*, 2117–2130. [[CrossRef](#)]
7. Yan, G.; Li, Z.; Galindo Torres, S.A.; Scheuermann, A.; Li, L. Transient two-phase flow in porous media: A literature review and engineering application in geotechnics. *Geotechnics* **2022**, *2*, 32–90. [[CrossRef](#)]
8. Wang, H.; Wang, X.P.; Yang, S.C.; Zhang, Z.; Jiang, F.S.; Zhang, Y.; Huang, Y.H.; Lin, J.S. Water erosion response to rainfall type on typical land use slopes in the red soil region of southern China. *Water* **2024**, *16*, 1076. [[CrossRef](#)]
9. Zhou, Y.H.; Shao, G.C.; Jiang, Y.H. Impact of Diverse Rainfall Patterns and Their Interaction on Soil and Water Loss in a Small Watershed within a Typical Low Hilly Region. *Water* **2024**, *16*, 372. [[CrossRef](#)]
10. Yang, H.; Wei, C.C.; Sun, G.H.; Tao, X.Q.; Wang, Y.T.; Xing, W.M. Responses of soil and ammonia nitrogen loss rates to hydraulic parameters under different slope gradients and rainfall intensities. *Water* **2024**, *16*, 230. [[CrossRef](#)]
11. Todisco, F. The internal structure of erosive and nonerosive storm events of interpretation of erosive processes and rainfall simulation. *J. Hydrol.* **2014**, *519*, 3651–3663. [[CrossRef](#)]
12. Fang, N.F.; Wang, L.; Shi, Z.H. Runoff and soil erosion of field plots in a subtropical mountainous region of China. *J. Hydrol.* **2017**, *552*, 387–395. [[CrossRef](#)]
13. Xie, Y.; Liu, B.Y.; Nearing, M.A. Practical thresholds for separating erosive and non-erosive storms. *Trans. ASAE* **2002**, *45*, 1843–1847. [[CrossRef](#)]
14. Wischmeier, W.H.; Smith, D.D. Rainfall energy and its relationship to soil loss. *Trans. Am. Geophys. Union* **1958**, *39*, 285–291. [[CrossRef](#)]
15. Jiang, Z.S.; Li, X.Y. Study on the rainfall erosivity and the topographic factor of predicting soil loss equation in the Loess Plateau. *Mem. NISWC Acad. Sin.* **1988**, *1*, 40–45. (In Chinese)
16. Zhang, X.K.; Xu, J.H.; Lu, X.Q.; Deng, Y.J.; Gao, D.W. A study on the soil loss equation in Heilongjiang Province. *Bull. Soil Water Conserv.* **1992**, *12*, 1–9. (In Chinese) [[CrossRef](#)]
17. Yang, Z.S. A study on erosive force of rainfall on sloping cultivated land in the northeast mountain region of Yunnan Province. *Sci. Geogr. Sin.* **1999**, *19*, 74–79. (In Chinese) [[CrossRef](#)]
18. Weng, X.R.; Ye, Y.; Ye, Y.; Zeng, B.S.; Long, X.J. Spatiotemporal characteristics of rainfall erosivity in Xiaonanxi Basin using multiple algorithms. *Trans. Chin. Soc. Agric. Eng.* **2022**, *38*, 143–150. (In Chinese) [[CrossRef](#)]
19. Zhang, Y.; Zhu, Q.K. Statistic analysis of erosive rainfall on the Loess Plateau. *J. Arid Land Resour. Environ.* **2006**, *20*, 99–103. (In Chinese)
20. Wang, W.Z. Study on the relations between rainfall characteristics and loss of soil in Loess Region III—Criteria for erosive rainfall. *Bull. Soil Water Conserv.* **1984**, *2*, 58–63. (In Chinese) [[CrossRef](#)]
21. Tian, X.M.; Li, F.Y.; He, X.W.; Wang, X.X.; Lu, X.Y.; Wang, L.Z.; Yu, Q. Study on daily erosive rainfall standard in the Poyang Lake Basin. *J. Soil Water Conserv.* **2021**, *35*, 185–189. (In Chinese) [[CrossRef](#)]
22. Gao, J.B.; Zhang, Y.B.; Zuo, L.Y. The optimal explanatory power of soil erosion and water yield in karst mountainous area. *J. Geogr. Sci.* **2023**, *33*, 2077–2093. [[CrossRef](#)]

23. Deng, O.; Li, M.; Yang, B.L.; Yang, G.B.; Li, Y.Q. Erosive rainfall thresholds identification using statistical approaches in a Karst Yellow Soil Mountain Erosion-Prone Region in Southwest China. *Agriculture* **2024**, *14*, 1421. [CrossRef]
24. Xie, Y.; Liu, B.Y.; Zhang, W.B. Study on standard of erosive rainfall. *J. Soil Water Conserv.* **2000**, *14*, 6–11. (In Chinese) [CrossRef]
25. Zhang, W.B.; Xie, Y.; Liu, B.Y. Rainfall erosivity estimation using daily rainfall amounts. *Sci. Geogr. Sin.* **2002**, *22*, 705–711. (In Chinese) [CrossRef]
26. Wu, C.G.; Lin, D.S.; Xiao, W.F.; Wang, P.C.; Ma, H.; Zhou, Z.X. Spatiotemporal distribution characteristics of rainfall erosivity in Three Gorges Reservoir Area. *Chin. J. Appl. Ecol.* **2011**, *22*, 151–158. (In Chinese)
27. Wang, W.Z. Study on the relations between rainfall characteristics and loss of soil in Loess Region. *Bull. Soil Water Conserv.* **1983**, *4*, 7–13. (In Chinese) [CrossRef]
28. Serio, M.A.; Carollo, F.G.; Ferro, V. Raindrop size distribution and terminal velocity for rainfall erosivity studies. *J. Hydrol.* **2019**, *576*, 210–228. [CrossRef]
29. Zhang, M.; Zhang, W.; Zhang, K.; Yu, Y.; Liu, L. Centennial scale temporal responses of soil magnetic susceptibility and spatial variation to human cultivation on hillslopes in Northeast China. *Soil Tillage Res.* **2023**, *234*, 105865. [CrossRef]
30. Tang, Q.Y.; Li, Y.H.; Hu, M.R.; Zhang, J.H.; Li, H.Y.; Fu, Z.Y.; Huang, S.Y.; Li, Y.L. Analysis of the spatiotemporal variation in heavy rainfall events in the Taihang Mountainous Region from 1973 to 2022. *J. Xinyang Norm. Univ. (Nat. Sci. Ed.)* **2024**, *37*, 524–531. (In Chinese) [CrossRef]
31. Chizhikova, N.; Yermolaev, O.; Golosov, V.; Mukharamova, S.; Saveliev, A. Changes in the regime of erosive precipitation on the European part of Russia for the period 1966–2020. *Geosciences* **2022**, *12*, 279. [CrossRef]
32. Ning, T.; Ma, X.Y.; Liu, S.M. Characteristics of erosive rainfall in the Yellow River Basin in Shanxi from 2000 to 2016. *Arid Zone Res.* **2020**, *37*, 1513–1518. (In Chinese) [CrossRef]
33. Cai, X.L.; Li, Q.; Hu, L.; Zhao, X.M. The spatial and temporal variations characteristic of erosive rainfall in the Yellow River basin during 1961–2010. *Adv. Mater. Res.* **2014**, *955*, 3269–3273. [CrossRef]
34. Zhang, B.; Tian, L.; He, C.S.; He, X.G. Response of erosive precipitation to vegetation restoration and its effect on soil and water conservation over China’s Loess Plateau. *Water Resour. Res.* **2023**, *59*, e2022WR033382. [CrossRef]
35. Huo, J.H.; Xiang, Y.P.; Qi, D.L.; Gao, G.S.; Chen, Q. Spatial and temporal variation of erosive precipitation in Qinghai Province from 1961 to 2018. *Desert Oasis Meteorol.* **2023**, *17*, 87–94. (In Chinese) [CrossRef]
36. Suo, X.Y.; Liu, Y.C.; Zhao, G.Y.; Tian, G.C.; Zhang, W.P.; Bai, L.F. Analysis on the change trend and abrupt change of rainfall and erosive rainfall in Tang-Qin region from 1960 to 2015. *Sci. Soil Water Conserv.* **2024**, *22*, 44–54. (In Chinese) [CrossRef]
37. Ministry of Water Resources, The People’s Republic of China. Chinese Soil and Water Conservation Bulletin. Available online: http://swcc.mwr.gov.cn/law/202404/t20240407_1741956.htm (accessed on 7 April 2024).
38. Ma, L.; Jiang, G.H.; Zuo, C.Q.; Qiu, G.Y.; Huo, H.G. Spatial and temporal distribution characteristics of rainfall erosivity changes in Jiangxi province over more than 50 years. *Trans. CSAE* **2009**, *25*, 61–68. (In Chinese) [CrossRef]
39. Cai, Z.Y.; Wang, Z.S.; Pan, Z.T. A numerical study on forecasting the Henan extraordinarily heavy rainfall event in August 1975. *Adv. Atmos. Sci.* **1992**, *9*, 53–62. [CrossRef]
40. Yang, L.; Liu, M.F.; Smith, J.A.; Tian, F.Q. Typhoon Nina and the August 1975 flood over central China. *J. Hydrometeorol.* **2017**, *18*, 451–472. [CrossRef]
41. Zhang, Q.H.; Li, R.M.; Sun, J.Z.; Lu, F.; Xu, J.; Zhang, F. A review of research on the record-breaking precipitation event in Henan Province, China, July 2021. *Adv. Atmos. Sci.* **2023**, *40*, 1485–1500. [CrossRef]
42. Jin, Z.; Yu, J.H.; Dai, K. Topographic elevation’s impact on local climate and extreme rainfall: A case study of Zhengzhou, Henan. *Atmosphere* **2024**, *15*, 234. [CrossRef]
43. Shi, B.L.; Zhu, X.Y.; Hu, Y.C.; Yang, Y.Y. Drought characteristics of Henan province in 1961–2013 based on Standardized Precipitation Evapotranspiration Index. *J. Geogr. Sci.* **2017**, *27*, 311–325. [CrossRef]
44. Zhang, J.J.; Guo, Z.F.; Li, Z.G. Research on time and spatial characteristics of flood and drought disasters risk in Henan. *J. Nat. Resour.* **2013**, *28*, 957–968. (In Chinese) [CrossRef]
45. Yang, Y.X.; Guo, Y.P.; Zhang, H.; Zhang, L.H.; Sang, J. Interpolation method of arable land quality grading based on barrier factors. *Trans. Chin. Soc. Agric. Mach.* **2019**, *50*, 157–165. (In Chinese) [CrossRef]
46. Wei, F.Y. *Climatological Statistical Diagnosis and Prediction Technology*; China Meteorological Press: Beijing, China, 1999. (In Chinese)
47. Sang, Y.F.; Wang, Z.G.; Liu, C.M. Applications of wavelet analysis to hydrology: Status and prospects. *Prog. Geogr.* **2013**, *32*, 1413–1422. (In Chinese) [CrossRef]

Disclaimer/Publisher’s Note: The statements, opinions and data contained in all publications are solely those of the individual author(s) and contributor(s) and not of MDPI and/or the editor(s). MDPI and/or the editor(s) disclaim responsibility for any injury to people or property resulting from any ideas, methods, instructions or products referred to in the content.